
CONTROLLING THE EWMA S^2 CONTROL CHART FALSE ALARM BEHAVIOR WHEN THE IN-CONTROL VARIANCE LEVEL MUST BE ESTIMATED

A PREPRINT

 **Sven Knoth**

Department of Mathematics and Statistics
Helmut Schmidt University
PO Box 700822
22008 Hamburg, Germany
knoth@hsu-hh.de

January 10, 2021

ABSTRACT

Investigating the problem of setting control limits in the case of parameter uncertainty is more accessible when monitoring the variance because only one parameter has to be estimated. Simply ignoring the induced uncertainty frequently leads to control charts with poor false alarm performances. Adjusting the unconditional in-control (IC) average run length (ARL) makes the situation even worse. Guaranteeing a minimum conditional IC ARL with some given probability is another very popular approach to solving these difficulties. However, it is very conservative as well as more complex and more difficult to communicate. We utilize the probability of a false alarm within the planned number of points to be plotted on the control chart. It turns out that adjusting this probability produces notably different limit adjustments compared to controlling the unconditional IC ARL. We then develop numerical algorithms to determine the respective modifications of the upper and two-sided exponentially weighted moving average (EWMA) charts based on the sample variance for normally distributed data. These algorithms are made available within an R package. Finally, the impacts of the EWMA smoothing constant and the size of the preliminary sample on the control chart design and its performance are studied.

Keywords Control charting; S^2 EWMA; phase I/II; false alarm probability

1 Introduction

Applying a surveillance scheme to monitor the stability of dispersion (homogeneity, scale or other related notions) is a common task used in industry to maintain, for example, the repeatability level of gauges, the uniformity of certain entities over time or space, the risk level of some financial asset, the stability of the variance underlying the control limits of a mean control chart and so forth. To provide an explicit example, we look at a scanning electron microscope (SEM) at a semiconductor company, where a battery of daily measurements is executed for the sake of repeatability monitoring. Typically, well-defined features (lines, spaces and so on) on a wafer are measured $n = 5$ times, and the resulting sample standard deviation is recorded on a Shewhart S chart — see Figure 1. Hence, it is not surprising that Shewhart, cumulative sum (CUSUM) and exponentially weighted moving average (EWMA) variance control charts are presented in popular textbooks, including [Montgomery \[2009\]](#), pages 259, 414 and 426, respectively, and [Qiu \[2013\]](#), pages 74, 146 and 198, respectively. Here, we wish to investigate methods for calibrating EWMA schemes based on the sample variance S^2 when the in-control (IC) level of the variance must be estimated based on a preliminary sample (phase I) of the IC data. The EWMA control chart was introduced by [Roberts \[1959\]](#) and gained much attention with and after [Lucas and Saccucci \[1990\]](#). The initial works on using EWMA charts for dispersion monitoring include

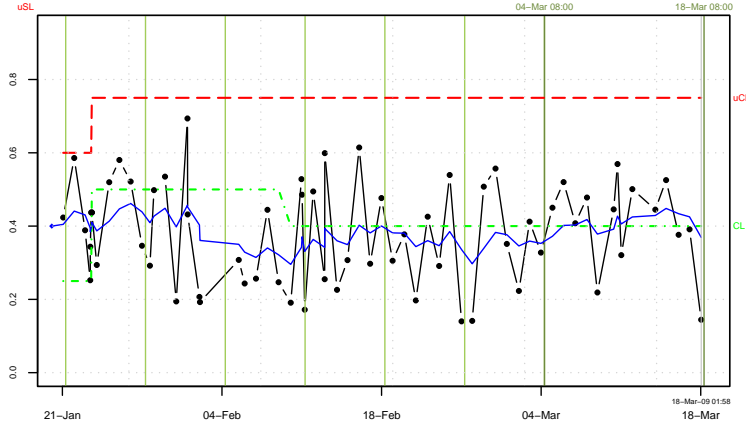


Figure 1: Shewhart S chart for monitoring the short-term repeatability of a scanning electron microscope (SEM); sample size $n = 5$; ordinate scale nm ; EWMA ($\lambda = 0.2$, blue) added.

Wortham and Ringer [1971], Sweet [1986], Domangue and Patch [1991], Crowder and Hamilton [1992], MacGregor and Harris [1993] and Chang and Gan [1994] — see Knoth [2005, 2010] for more details.

With regard to EWMA charts, Jones et al. [2001] started the analysis of using estimated parameters instead of merely assuming known ones. It became, for control charts in general, an important topic in the statistical process control (SPC) literature over the course of the last 20 years, and Jensen et al. [2006] and Psarakis et al. [2014] have provided detailed surveys on this subject. Typically, it is assumed that the parameters are estimated through m phase I samples, each of size n , which means that nearly all the performance measures used for control charts become uncertain. For example, the well-known average run length (ARL; expected number of samples until the chart signals) becomes a random variable. Two frameworks are commonly used to deal with this additional uncertainty. In the first framework, an unconditional form is calculated by applying a total probability mechanism. We will refer to this form as the unconditional ARL — others use notions such as the marginal or mean ARL. Below, we will illustrate that controlling the unconditional IC ARL induces some puzzling side effects. The second framework started with Albers and Kallenberg [2001, 2004a,b], who considered probabilistic bounds for performance measures, such as the conditional ARL. More recent contributions from, for instance, Capizzi and Masarotto [2010], Jones and Steiner [2011] and Gandy and Kvaløy [2013], have stimulated a series of additional publications employing this approach. A popular motivation for this guarantee-a-minimum IC ARL is that it incorporates appropriately the so-called practitioner-to-practitioner variability. This framework has been discussed extensively for Shewhart charts monitoring the normal variance in Epprecht et al. [2015], Guo and Wang [2017], Goedhart et al. [2017], Faraz et al. [2015], Faraz et al. [2018], Aparisi et al. [2018], and Jardim et al. [2019]. Most of the latter works derived numerical procedures for calculating the limit adjustments, which is much more difficult for CUSUM and EWMA control charts, where Monte Carlo simulations (bootstrapping for the phase I dataset) are typically used. Thus, it is not surprising that nothing has been published on monitoring the normal variance for CUSUM and EWMA charts as of yet. Moreover, there are further problems with this framework. First, it is truly difficult to communicate the probabilistic bound for the random (conditional) IC ARL to a practitioner. Second, the modified limits are commonly quite wide, resulting in a prolongation of the detection delays. Therefore, Capizzi and Masarotto [2020] proposed to re-estimate the modification regularly during phase II to tighten the limits. Third, the calculations of the actual modifications for CUSUM and EWMA charts are involved and time consuming. While the last problem will be probably be solved soon, the other problems persist. Hence, we propose a different approach. We widen the limits of an EWMA S^2 chart by assuring a certain unconditional IC run length (RL) quantile. Later, we will see that aiming at an unconditional IC RL quantile leads to a widening of the limits, whereas deploying the unconditional IC ARL can tighten them.

Contrary to the case of the Shewhart variance chart, there are only a few contributions dealing with EWMA variance charts under parameter uncertainty, namely, Marvelakis and Castagliola [2009], and more recently, Zwetsloot et al. [2015] and Zwetsloot and Ajadi [2019]. All together control the unconditional IC ARL. Marvelakis and Castagliola [2009] investigated EWMA charts utilizing $\ln S^2$. From their unconditional out-of-control (OOC) ARL results we pick a few, in order to discuss what we call the unconditional ARL puzzle. In their Table 2, unconditional OOC ARL numbers for an upper EWMA $\ln S^2$ with an unconditional IC ARL of 370.4 were given. We provide these numbers in Table 1, for $\lambda = 0.01$, $n = 4$ and $m \in \{10, 20, 40, 80\}$ as well as $m = \infty$ (known parameter case). These results include a non-remediable issue, namely, the favorable ARL values for small m suggest that small phase I samples should be utilized. In other words, the more reliable the estimate of the unknown σ_0^2 (including in the known parameter

m	10	20	40	80	∞
ARL	13.1	16.3	18.9	20.5	22.6

Table 1: Side effects of using the unconditional ARL as a calibration target (IC 370.4): Unconditional OOC ARL values (standard deviation increased by 20%) for several phase I sizes, m ; sample size $n = 5$; EWMA $\ln S^2$ chart with $\lambda = 0.01$.

case), the longer one has to wait to detect this specific increase, that is, controlling the unconditional IC ARL tightens the limits substantially, resulting in this uncommon improvement in the detection behavior. However, this tightening greatly increases the probability of early false alarms. The heavy tail of the unconditional IC RL distribution enlarges the corresponding mean (the unconditional IC ARL), while the probability of low RL values becomes larger at the same time. Later on, we will discuss this issue in more detail. Zwetsloot et al. [2015] utilized the unconditional ARL to adjust their limits and obtained similar OOC ARL anomalies. Neither paper discussed these patterns. Yet, Chakraborti [2007] indicated that focusing on the unconditional ARL is dangerous. In sum, controlling the unconditional IC ARL is not the way to go.

It should be added that the ARL paradigm has been criticized apart from studying the estimation uncertainty influence on control charts limits. For example, Yashchin [1985] wrote: “*Though ARL is probably meaningful in the off-target situation, it can be highly misleading when the on-target case is under study (primarily because the set of possible CUSUM paths includes ‘too many’ extremely ‘short’ members)*”. For a more recent critique, see Mei [2008] or Kuhn et al. [2019] and the references therein. Yashchin [1985] also reported (for the competing CUSUM control chart): “*In general, the user of a CUSUM scheme probably feels uneasy about specifying a particular ARL for the on-target situation; what he typically wants is that the scheme will not generate a false alarm within a certain period of time (say, a shift) with probability of at least, say, 0.99.*”. This last passage refers to our design principle.

In sum, we study and propose two key features: (i) A novel control chart design rule for incorporating estimation uncertainty that uses neither the misleading unconditional ARL nor the too conservative guarantee-a-minimum conditional ARL. We control the unconditional false alarm probability via an unconditional IC RL quantile. (ii) We utilize a numerical procedure that is more accurate than the Markov chain approximation [Maravelakis and Castagliola, 2009] and much quicker than Monte Carlo-based procedures [Zwetsloot et al., 2015].

The paper proceeds as follows: In Section 2, we introduce the EWMA S^2 chart in detail and illustrate the peculiarities that emerge when some estimate of the IC level is simply plugged in. In addition, we elucidate the deceptive concept of adjusting the unconditional IC ARL. Afterwards, in Section 3, we describe our novel approach and the numerical algorithm used to obtain the unconditional RL quantiles. Eventually, in Section 4, we use this machinery to study the impact of the actual EWMA design (smoothing constant) and of the phase I size m on both the resulting control limit modification and the detection performance. In the last section, we present our concluding discussion.

2 EWMA S^2 under in-control level uncertainty

EWMA schemes utilizing the sample variance S^2 are one type of EWMA chart monitoring dispersion. Competitors include $\ln S^2$, which is used in Crowder and Hamilton [1992]; S , as in, for example, Mittag et al. [1998]; the sample range R , which is found in Ng and Case [1989]; and $a + b \ln(S^2 + c)$, as in Castagliola [2005]. Note that all these papers, including ours, consider normally distributed data. There are several reasons to prefer S^2 . First, it is an unbiased estimator of the variance. Second, EWMA S^2 frequently exhibits the best detection performance – refer to Knoth [2005, 2010]. Third, the calculation is more feasible if all the estimation and monitoring is done with S^2 .

Now, let $\{X_{ij}\}$ be a sequence of subgroups of independent and normally distributed data. Each subgroup i consists of $n > 1$ observations X_{i1}, \dots, X_{in} . As usual, we assume that the phase I data come from a stable process and that the variance change occurs at the beginning of the monitoring period or never. Calculating the running sample variance S_i^2 , $i = 1, 2, \dots$,

$$S_i^2 = \frac{1}{n-1} \sum_{j=1}^n (X_{ij} - \bar{X}_i)^2, \quad \bar{X}_i = \frac{1}{n} \sum_{j=1}^n X_{ij},$$

we feed the EWMA iteration sequence in the usual way:

$$Z_i = (1 - \lambda)Z_{i-1} + \lambda S_i^2, \quad Z_0 = z_0 = \sigma_0^2.$$

The EWMA smoothing constant, λ , is in the interval $(0, 1]$ and controls the detection sensitivity. The EWMA sequence $\{Z_i\}$ is initialized with the IC variance level, σ_0^2 . Here, we must estimate σ_0^2 anyway.

We want to detect increases or two-sided changes in the variance level. Hence, the following (alarm) stopping times are utilized:

$$\begin{aligned} L_{\text{upper}} &= \min \{i \geq 1 : Z_i > c_u\}, \\ L_{\text{two}} &= \min \{i \geq 1 : Z_i > c_u \text{ or } Z_i < c_l\}. \end{aligned}$$

Note that introducing a lower reflection barrier to the upper scheme would diminish the inertia effects — see [Woodall and Mahmoud \[2005\]](#) for more details. It would, however, also increase the complexity and dismantle the rolling estimate feature of the plain EWMA sequence Z_i . Moreover, the inertia effect is less pronounced for a S^2 -based chart with the intrinsic lower limit 0 compared to a mean chart, which would be unbounded from below. Therefore, we prefer the simpler design without a lower barrier.

Typically, the control limits are chosen to provide a pre-defined IC ARL, for example, by aiming for $E(L) = 500$. In the case of a known IC variance σ_0^2 , there is a rich body of literature on calculating the ARL and solving the inverse task of determining control limits for a given IC ARL value. In this paper, we use algorithms from [Knoth \[2005, 2007\]](#) to compute the ARL, RL quantiles, and RL distribution for an EWMA S^2 control chart. The related R package `spc` offers functions that make this calculation easy.

We will start with a typical situation: Sample size $n = 5$, EWMA constant $\lambda = 0.1$ and target IC ARL 500. This setup calls for thresholds $c_l = 0.6259$ and $c_u = 1.5496$ for the two-sided EWMA alarm design, and the threshold $c_u = 1.4781$ for the upper EWMA alarm design. For the former, we decided to use an ARL-unbiased design. This notion was introduced by [Pignatiello et al. \[1995\]](#) and [Acosta-Mejía and Pignatiello \[2000\]](#), but the phenomenon was discussed earlier in [Uhlmann \[1982\]](#) and [Krumbholz \[1992\]](#) (both in German), in [Champ and Lowry \[1994\]](#) and, presumably, in further publications. For more details, refer to the more recent [Knoth \[2010\]](#) and [Knoth and Morais \[2015\]](#). In a nutshell, ARL-unbiased designs render the ARL maximum at the IC level; in this case, σ_0^2 . For the unknown parameter case, [Guo and Wang \[2017\]](#) provided results recently for ARL-unbiased Shewhart S^2 charts while guaranteeing a minimum conditional IC ARL.

In this paper, we use a phase I reference dataset consisting of m samples of size n and build the estimate, that is, the pooled sample variance

$$\hat{\sigma}_0^2 = \frac{1}{m} \sum_{i=1}^m s_i^2, \quad (1)$$

where s_i^2 denotes the sample variance of the pre-run sample $i = 1, 2, \dots, m$. For a discussion on appropriate estimators of the unknown σ_0^2 , we refer to [Mahmoud et al. \[2010\]](#), [Zwetsloot et al. \[2015\]](#) and [Saleh et al. \[2015\]](#). Here, we focus on the above “natural” estimator because it is unbiased (no further corrections are needed) and its distribution is readily available, that is, a χ^2 distribution with $m \times (n - 1)$ degrees of freedom. [Zwetsloot et al. \[2015\]](#) mentioned that “*under in-control data the EWMA control charts show similar performance across all estimators*,” where “in-control” refers to an uncontaminated phase I. Replacing this “natural” estimator with a more robust [\[Zwetsloot et al., 2015\]](#) or otherwise more suitable estimator does not change the framework described below, but doing so makes the calculations more complicated. We want to emphasize, however, that all our theoretical and numerical results make use of the pooled variance estimator (1). To use the aforementioned estimate means that the observed X_{ij} are standardized, resulting in $\tilde{X}_{ij} = X_{ij}/\hat{\sigma}_0$. In consequence, we run an EWMA chart design for $\sigma_0^2 = 1 = z_0$ with the limits mentioned above. Now, we wish to study the impact on the unconditional cumulative distribution function (CDF) $P(L \leq l)$ depending on the phase I sample size m . Note that $P(L \leq l)$ covers two sources of uncertainty: (i) phase I estimation, and (ii) phase II monitoring. Applying the numerical algorithms described in the next section, in [Figure 2](#), we illustrate this CDF for several phase I sizes assuming a known σ_0^2 during setup. The graphs in the two-sided case feature simple patterns, namely, the smaller the phase I sample size m , the higher the probability that a false alarm is flagged by l for any $l \in \{1, 2, \dots\}$. In the case of the upper chart, this relation remains valid for early values of $l \leq 350$ (roughly the original RL median) only. For large values, it is reversed. For small phase I sample sizes, such as $m \leq 50$, the unconditional IC RL distribution has heavy tails. For instance, the unconditional probability $P(L > 10^5)$ is roughly 0.1 and 0.02 for $m = 10$ and $m = 30$, respectively. Given that, for example, [Zwetsloot et al. \[2015\]](#) truncate their Monte Carlo simulations at $l = 30\,000$, some potential problems with the unconditional IC ARL and even some IC RL quantiles might be hidden. Nonetheless, using the unconditional IC ARL to adjust the limits is dangerous because the particular tails distort the expectation and explains the peculiar numbers in [Table 1](#) taken from [Maravelakis and Castagliola \[2009\]](#). Hence, calibrating upper EWMA variance charts by aiming for a certain unconditional IC ARL is misleading.

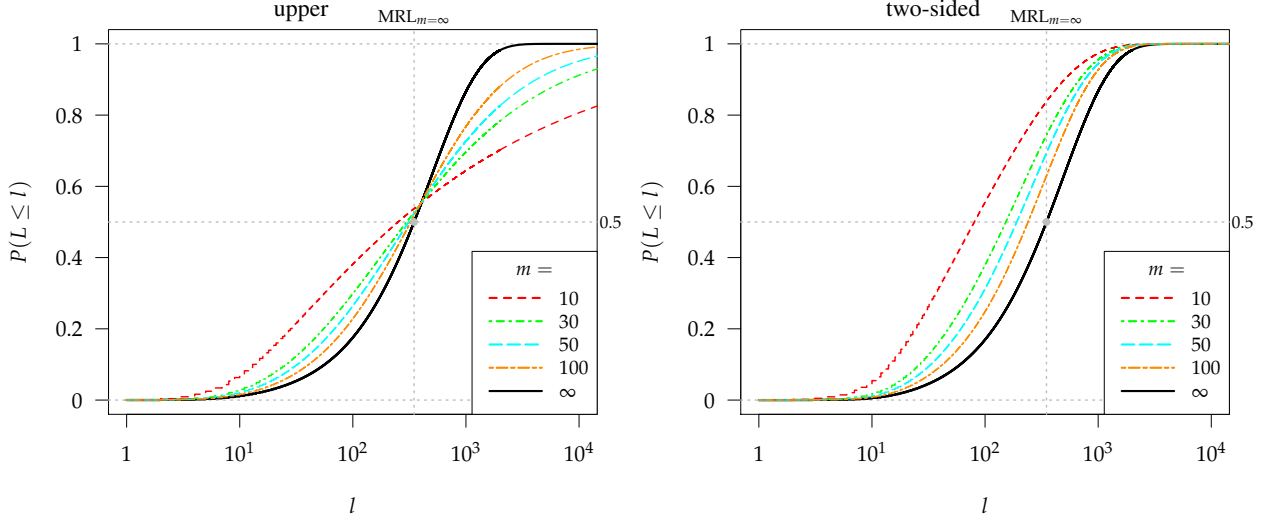


Figure 2: Unconditional IC RL CDF for the EWMA ($\lambda = 0.1$) S^2 ($n = 5$), phase I size m , unadjusted case.

3 Numerical algorithm and actual adjustment

We want to adjust the EWMA control limits c_u and c_l (just the two-sided case) in order to achieve

$$P(L \leq \bar{l}) = \alpha, \quad (2)$$

where $P(\cdot)$ is the unconditional IC CDF of the RL L . In other words, we alter the limits so that \bar{l} becomes the unconditional IC RL α quantile. Recall that there is a direct link between the ARL and an RL quantile of order α for Shewhart charts with known IC parameters: $RL_\alpha = \lceil \ln(1 - \alpha) / \ln(1 - 1/ARL) \rceil$. This simple formula remains approximately valid for EWMA S^2 charts in the IC case if σ_0^2 is known: The median RL (MRL) is equal to 348 and $349 \approx 347 = \lceil \ln(0.5) / \ln(1 - 1/500) \rceil$ with an ARL = 500 for the upper and two-sided EWMA S^2 charts, respectively, in Figure 2. However, this simple relationship is lost, if we deal with the unconditional IC CDF. In the beginning of Section 4, we provide some illustrations of this phenomenon. This behavior is not surprising because the unconditional IC CDF is very different from the simple geometric distribution we exploited for the Shewhart chart RL statement. Using our rule (2), we tackle the problems observed in Figure 2 directly. Appropriate choices of α are those that are smaller than 0.5 (we will use $\alpha = 0.25$), while \bar{l} could be either derived from the ARL and RL quantile relationship for known σ_0^2 or set manually, as in $\bar{l} = 1000$, which is used for a typical control chart in practice. Next, we develop an algorithm to calculate the unconditional CDF and use the result to solve the implicit function (2) numerically with the secant rule.

For calculating the unconditional CDF, we adhere to Waldmann [1986], who proposed the idea for EWMA control charts being used to monitor a normal mean with known IC parameters. We start with the upper chart, which only requires an adjustment to its upper limit c_u . Let $p_l(z) = P(L > l \mid Z_0 = z)$ denote the survival function (SF) of the RL for known σ_0^2 and starting values $Z_0 = z$. Adding further arguments, such as the actual variance σ^2 and control limit c_u , we produce its unconditional version

$$p_{l,\text{unc.}}(z; \sigma^2, c_u) = \int_0^\infty f_{\delta_0^2}(s^2) p_l(z; \sigma^2/s^2, c_u) ds^2 \quad , \quad l = 1, 2, \dots \quad (3)$$

The formula (3) is related to (16) in Jones et al. [2001]. Note that only one integral is needed and that we consider the SF instead of the probability mass function of the RL L . To increase the computational speed for (3), the geometric tail behaviors [Waldmann, 1986] of $p_l(z; \sigma^2/s_i^2, c_u)$ at each quadrature node s_i^2 are (for large l) exploited individually. Unfortunately, it is lacking for $p_{l,\text{unc.}}(z; \sigma^2, c_u)$, as has been mentioned previously in, for example, Psarakis et al. [2014]. The density $f_{\delta_0^2}(\cdot)$ is roughly the probability density function (PDF) of a chi-square distribution (multiply the degrees of freedom). The numerical implementation for $p_l(\cdot)$ is taken from Knoth [2007]. Because its presentation is not easily accessible, we provide some necessary details here. We begin with the transition (from z_0 to z) density of the EWMA S^2 sequence as follows:

$$\delta(z_0, z) = \frac{1}{\lambda} f_{\chi^2; n-1} \left(\frac{n-1}{\sigma^2} \left[\frac{z - (1-\lambda)z_0}{\lambda} \right]^2 \right) \frac{n-1}{\sigma^2},$$

where $f_{\chi^2; n-1}()$ and $F_{\chi^2; n-1}()$ denote the PDF and CDF, respectively, of a chi-square distribution with $n - 1$ degrees of freedom. Then we obtain the following recursions for the SF $p_l(z; \dots) := p_l(z; \sigma^2/s^2, c_u)$:

$$p_1(z_0; \dots) = \int_{(1-\lambda)z_0}^{c_u} \delta(z_0, z) dz = F_{\chi^2; n-1} \left(\frac{n-1}{\sigma^2} \left[\frac{c_u - (1-\lambda)z_0}{\lambda} \right] \right), \quad (4)$$

$$p_l(z_0; \dots) = \int_{(1-\lambda)z_0}^{c_u} p_{l-1}(z; \dots) \delta(z_0, z) dz \quad , \quad l = 2, 3, \dots \quad (5)$$

A common approach to approximating the integral recursions is to replace the integrals by quadratures [Jones et al., 2001]. Fixed quadrature grids, however, have lower integral limit issues since this limit, $(1 - \lambda)z_0$, depends on the argument $p_l(z_0; \dots)$, see Knoth [2005] for a more thorough analysis. Another idea is to apply a collocation type of procedure, as in Knoth [2007], Shu et al. [2013] and Huang et al. [2013], who transferred the collocation principle from the ARL integral equation in Knoth [2005] to integral recursions. Essentially, for every $l = 2, 3, \dots$, we approximate

$$p_l(z; \dots) \approx \sum_{s=1}^N g_{ls} T_s^*(z),$$

with N suitably shifted Chebyshev polynomials $T_s^*(z)$, $s = 1, 2, \dots, N$ (the $T_s()$ are the unit versions),

$$\begin{aligned} T_s^*(z) &= T_{s-1}((2z - c_u)/c_u) \quad , \quad z \in [0, c_u], \\ T_s(z) &= \cos(s \arccos(z)) \quad , \quad z \in [-1, 1]. \end{aligned}$$

Then we pick N nodes z_r defined as (roots of $T_N(z)$ shifted to the interval $[0, c_u]$)

$$z_r = \frac{c_u}{2} \left[1 + \cos \left(\frac{(2i-1)\pi}{2N} \right) \right] \quad , \quad r = 1, 2, \dots, N,$$

and consider the following recursion on the grid $\{z_r\}$, $l = 2, 3, \dots$,

$$\sum_{s=1}^N g_{ls} T_s(z_r) = \sum_{s=1}^N g_{l-1,s} \int_{(1-\lambda)z_r}^{c_u} T_s(z) \delta(z_r, z) dz.$$

These definite integrals must be determined numerically. Because they do not depend on l (only on s and r), we calculate them once and store them in an $N \times N$ matrix. Using this matrix and the starting vector $\mathbf{g}_1 = (g_{11}, g_{12}, \dots, g_{1N})'$ derived from (4), we build a numerical approximation for (5) that provides a highly accurate numerical presentation of the SF $p_l(z_0; \dots)$ used in (3) to determine the unconditional CDF of the RL L . The resulting SF $p_{l,\text{unc.}}(z_0; \sigma^2, c_u)$ is implemented in the R package `spc` as the function `sewma.sf.prerun(1, lambda, 0, cu, sigma, n-1, m*(n-1), hs=z0, sided="upper")`, see the Appendix for an example of an application. In Figure 3, we compare the approximation accuracies of the collocation and the Markov chain framework. We investigate the EWMA S^2 with $\lambda = 0.1$ and sample size $n = 5$ and set $\bar{l} = 10^3$ and $\alpha = 0.25$, resulting in $c_u = 1.719846$. The integral in (3) is approximated by the Gauß-Legendre quadrature with 60 nodes, while replacing the upper limit ∞ by 1.773 ($1 - 10^{-10}$ quantile of a chi-square distribution with $m \times (n - 1) = 200$ degrees of freedom divided by 200). This integral is deployed for the SF $p_{l,\text{unc.}}(z_0; \sigma^2, c_u)$ and the unconditional ARL as well. The matrix dimension N indicates the size of the collocation basis (see above) and the number of transient states of the Markov chain. From the two figures, we conclude that collocation with $N = 50$ yields much higher accuracy than the Markov chain with $N = 500$. For calculating $p_{l,\text{unc.}}(1; 1, c_u)$, collocation needs about 1 second for $N = 50$, while the Markov chain approximation requires 3, 6, 15 and 22 seconds for $N = 200, 300, 400$ and 500, respectively. Eventually, we want to solve (2) as an implicit, continuous function of the upper limit c_u numerically by executing a secant rule-type algorithm. The starting values will be slightly increased limits from the known parameter case.

Turning to the two-sided case, we face additional problems. First, the numerical procedure (collocation proceeds “piece-wise” now) becomes more involved and therefore more time consuming. The general idea follows what has been outlined above, so we will skip the details [for an elaborated description see Knoth, 2005]. The second problem is that we must now determine two limits, c_l and c_u , without an intrinsic symmetric limit design, unlike what we encountered for monitoring the normal mean. Hence, we must either deploy the symmetric design $\sigma_0^2 \pm c$ by simply ignoring the asymmetric behavior of EWMA S^2 or enforce something similar to the ARL-unbiased design used in the known-parameter case. We try two concepts: (i) make the unconditional $P_\sigma(L \leq \bar{l})$ minimal in $\sigma = \sigma_0 = 1$

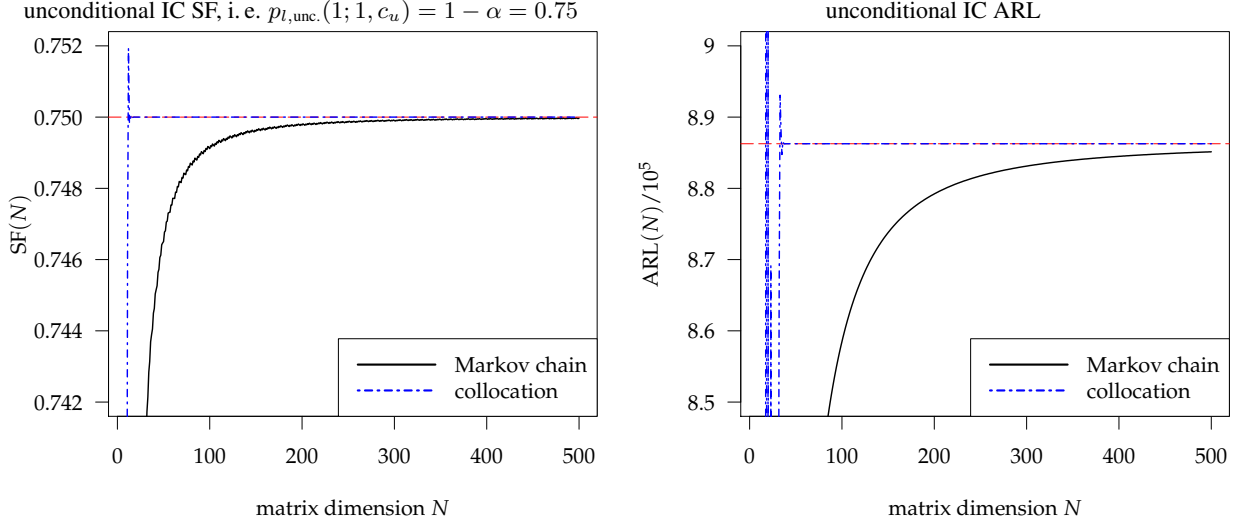


Figure 3: Approximation accuracies of the Markov chain and collocation for EWMA ($\lambda = 0.1$) S^2 ($n = 5$), phase I size $m = 50$, $P_{IC}(L \leq 10^3) = 0.25$.

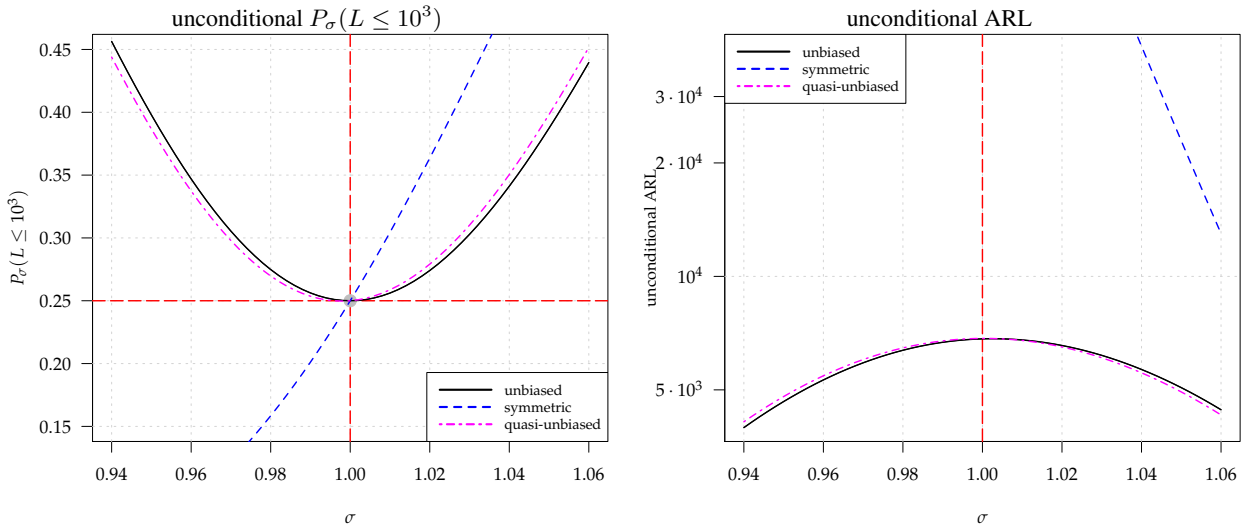


Figure 4: Judging “unbiasedness” in the two-sided case: The unconditional $P_\sigma(L \leq 10^3)$ and ARL as functions of the actual standard deviation σ for EWMA ($\lambda = 0.1$) S^2 ($n = 5$), phase I size $m = 50$, $P_{IC}(L \leq 10^3) = 0.25$.

(with no loss of generality) — denoted henceforth as the “unbiased” version, and (ii) perform (i) for the known parameter case (much faster) and expand the resulting limits (c_l^∞, c_u^∞) by incorporating the correction $\xi > 1$ via $c_l = c_l^\infty / \xi$ and $c_u = c_u^\infty \cdot \xi$ so that we achieve the unconditional $P_{IC}(L \leq \bar{l}) = \alpha$ — we label this method as the “quasi-unbiased” method. All three approaches are illustrated in the following example: $\lambda = 0.1$, $\bar{l} = 10^3$, $\alpha = 0.25$, $n = 5$ and $m = 50$. In all cases, we determine the new limits numerically by essentially applying the secant rule (a more sophisticated implementation is the function `uniroot()` in R). The resulting limits are (0.280153, 1.719847) (half width $c = 0.719847$), (0.528670, 1.824855) and (0.526394, 1.817301) (correction factor $\xi = 1.065821$ applied to $(c_l^\infty, c_u^\infty) = (0.561042, 1.705071)$) for the symmetric, unbiased and quasi-unbiased approaches, respectively. In Figure 4, we illustrate the resulting profiles for $P(L \leq 10^3)$ and the ARL as functions of the actual standard deviation σ . For both, we deployed the unconditional distribution. Note that the simple symmetric design exhibits profiles (SF and ARL) that are far from being unbiased. Moreover, the unconditional OOC ARL is very large for $\sigma < \sigma_0 = 1$ (the lower limit is much smaller than those of the two competitors). Hence, from this point forward, we will drop the symmetric limit design. The more sophisticated procedures feature rather equal profiles. In the sequel, we will apply the unbiased approach to be on the safe side. However, because it needs considerably more computing time than the

quasi-unbiased scheme, we recommend the latter for daily practice. We should note that the large unconditional ARL values are the result of the special setup utilized here. For instance, when σ_0^2 is known, we observe an IC ARL of about 3 450, which is then inflated to about 6 800 by two sources: the widened limits and enlarged tails of the unconditional RL distribution. To achieve smaller values, $\bar{l} = 10^3$ should be decreased or $\alpha = 0.25$ should be increased. It should be noted that that using $\sigma_0 = 1$ does not violate the generality of our results. Hence, σ will refer to the standardized version $\sigma_0 = 1$. For example, $\sigma = 1.2$ means that the OOC standard deviation is 20% larger than its (unknown) IC counterpart. Finally, we should emphasize that the unconditional $\alpha = 0.25$ RL quantile $\bar{l} = 10^3$ differs substantially from measures such as “ $Percentile_{\text{marginal}}$ ” [Zhang et al., 2014], where the RL quantile for known σ_0^2 replaces $p_l(z; \dots)$ in (3). This weighted average over all conditional RL quantiles is much larger. For example, we obtain 244 325 for $\alpha = 0.25$. The exception is the unconditional ARL. To calculate it, we could utilize either (3) and plug in the conditional means or sum up $p_{l,\text{unc.}}(z; \dots)$ over all l , which is just the expectation of the unconditional RL distribution. It remains somewhat unclear what exactly is being measured with $Percentile_{\text{marginal}}$.

After deriving these quite involved algorithms, we use them to illustrate the dependence of c_u on the phase I size m . Utilizing our setup with $\bar{l} = 1000$, $\alpha = 0.25$ and EWMA’s $\lambda = 0.1$, we start with the limits for known σ_0^2 as

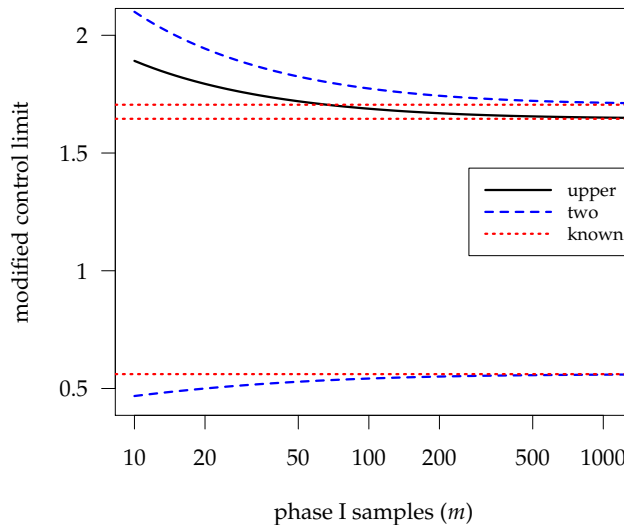


Figure 5: Modified control limits for $P_{\text{IC}}(L \leq 10^3) = 0.25$, upper and two-sided EWMA ($\lambda = 0.1$) S^2 ($n = 5$), m varies.

a benchmark — $c_u = 1.6453$ and ($c_l = 0.5610$, $c_u = 1.7051$) for the upper and two-sided cases, respectively. For realistic values of phase I sample sizes m between 10 and 1 000, we obtain widened limits, as can be seen in Figure 5. From the profiles, we conclude that the widening is less pronounced than might be expected. From sizes $m = 50$ on, the resulting limits on the control chart device in use would not really differ from the ideal case in which σ_0^2 is known.

Applying these new control limits changes the CDF profiles from those in Figure 2 to the ones presented in Figure 6. All profiles go through the point (\bar{l}, α) by construction, of course. However, we observe that the smaller the phase size m , the more likely the very early false alarms.

Widening the limits allows poor false alarm levels to be dealt with. However, the behavior in the OOC case has deteriorated. Using the limits from $P_{\text{IC}}(L \leq 1000) = 0.25$, we show the unconditional CDFs for selected OOC cases ($\sigma_1 \in \{0.8, 1.2\}$) in Figure 7. Note the poor detection behavior for smaller values of m . For $m < 50$, it is possible that the variance change will remain undetected over the entire planned monitoring time span ($\bar{l} = 1000$ observations). It is even worse for the two-sided case. Based on the profiles in Figure 7, we would recommend phase I sizes of at least 100. For more details, we refer the reader to the next section.

In order to provide some more familiar representations and at least get an idea of the detection speed, we add some unconditional ARL values to the OOC case in Figure 8. The differences in the benchmark case are considerably large for $m < 100$ and become negligible only for $m > 200$. Hence, there is an obvious price to pay if we account for the phase I estimation uncertainty when calibrating the chart. Because the false alarm behavior is really important for practical control charting in industry, the calibration strategy utilizing $P(L \leq \bar{l}) = \alpha$ seems to be passable despite these side effects. Note that the even more conservative approach of guaranteeing a minimum conditional IC ARL yields substantially larger unconditional OOC ARL results.

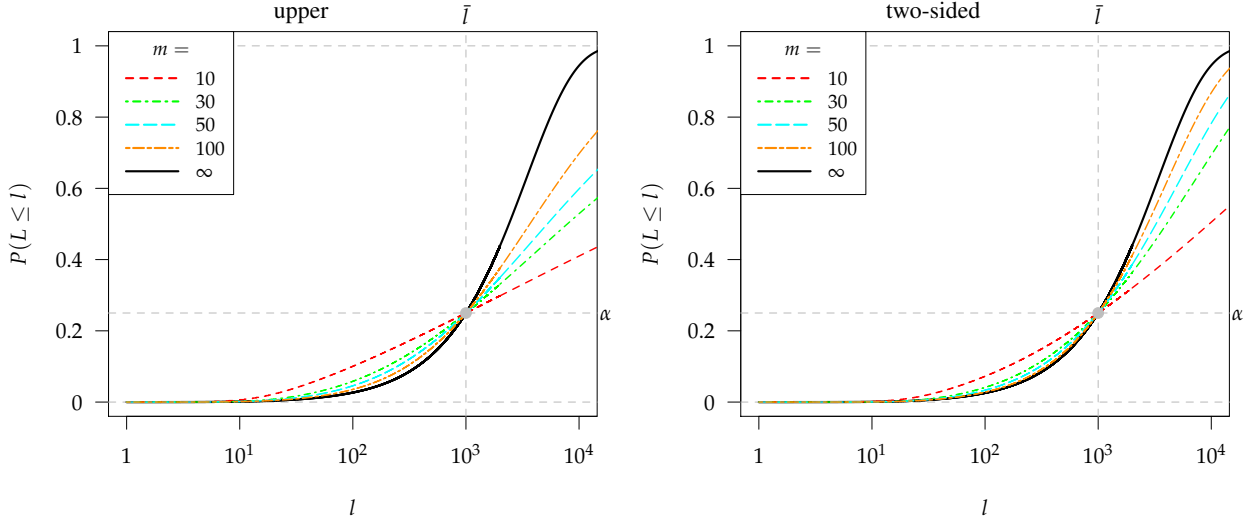


Figure 6: Unconditional IC RL CDF for EWMA ($\lambda = 0.1$) S^2 ($n = 5$), phase I size m , $P_{IC}(L \leq 10^3) = 0.25$.

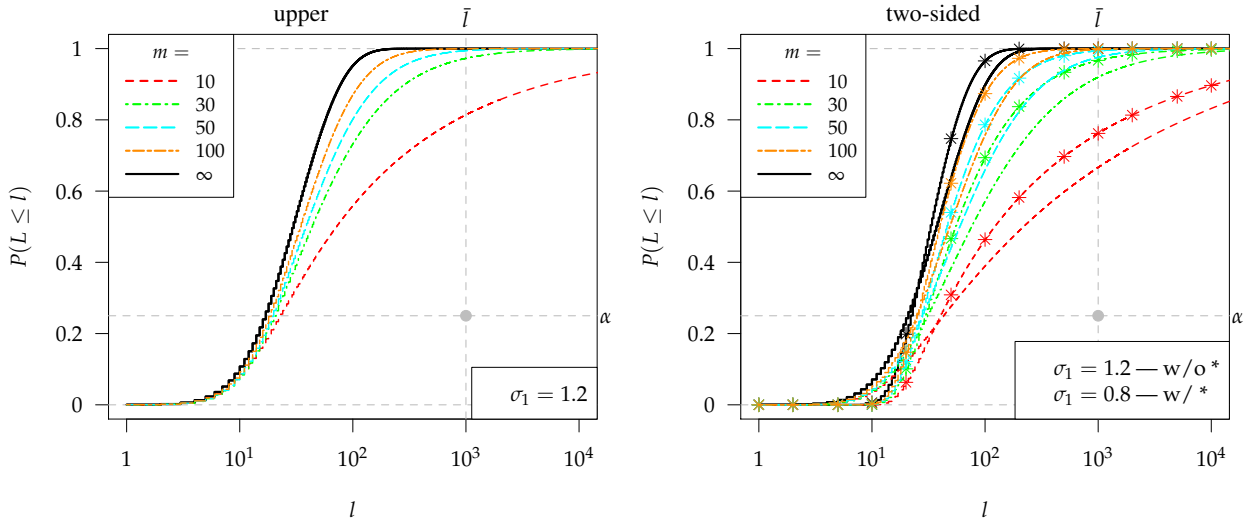


Figure 7: Unconditional OOC RL CDFs for EWMA ($\lambda = 0.1$) S^2 ($n = 5$), phase I size m , $P_{IC}(L \leq 10^3) = 0.25$.

4 Sensitivity and competition

To reconcile the common IC ARL user to this method, we investigate the selection of the monitoring horizon \bar{l} and false alarm probability α for a given IC ARL of, for example, 500 and its impact on the actual adjustment of the control limits accounting for the estimation uncertainty. To begin with, we set $\alpha = 0.5$ to ensure that the IC median run length (MRL) 348 (349 in the two-sided case) is achieved. From Figure 9(a), we conclude that focusing on the unconditional ARL yields the smallest c_U , followed by simply utilizing the c_U value for known σ_0^2 and, finally, the unconditional MRL (median RL) design. Obviously, downsizing the upper limit seems to be counter-intuitive and results in more false alarms than intended. The slight increase of c_U from the known σ_0^2 case to the MRL-conserving approach offers a cautious and effective way of dealing with the estimation uncertainty. By changing α (or \bar{l}), we can see that for all $\alpha < 0.56$, the modified c_U is larger than for known σ_0^2 . In addition, decreasing α (and \bar{l} , accordingly) increases c_U further (except for very small α). Of course, proper choices of α are 0.5 or smaller. In the two-sided case, all designs securing some unconditional measure widen the original limits. In Figure 9(b), we plot only the upper value c_U . For $\alpha < 0.75$, the unconditional RL quantiles induce wider limits than the unconditional ARL design. In summary, deciding on a reasonable combination (\bar{l}, α) provides plausible and effective limit adjustments that can overcome the estimation uncertainty distortions.

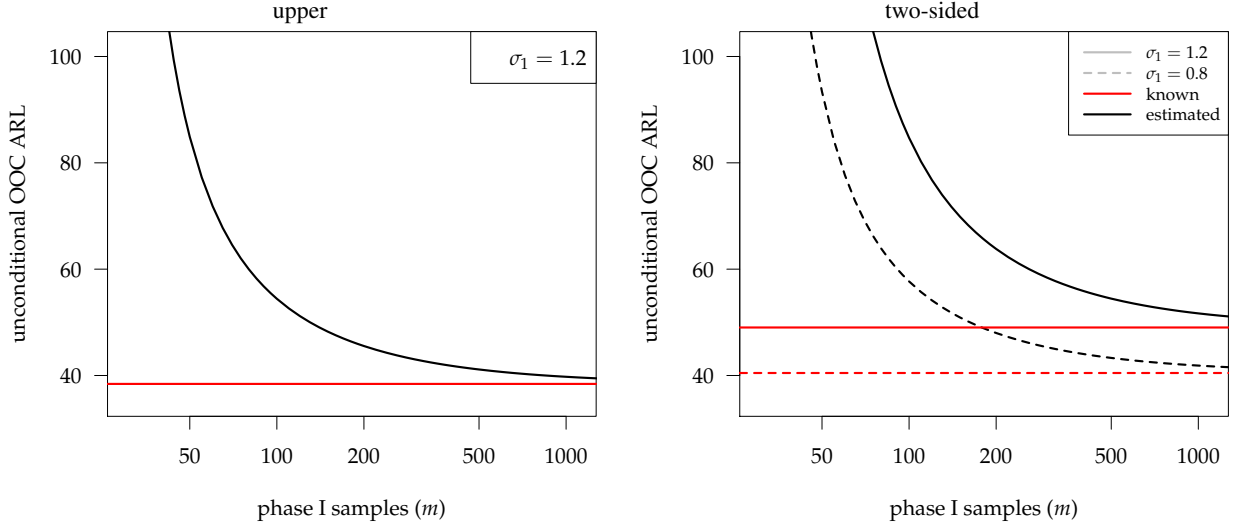


Figure 8: Unconditional OOC ARLs for EWMA ($\lambda = 0.1$) S^2 ($n = 5$) vs. phase I size m , $P_{IC}(L \leq 10^3) = 0.25$.

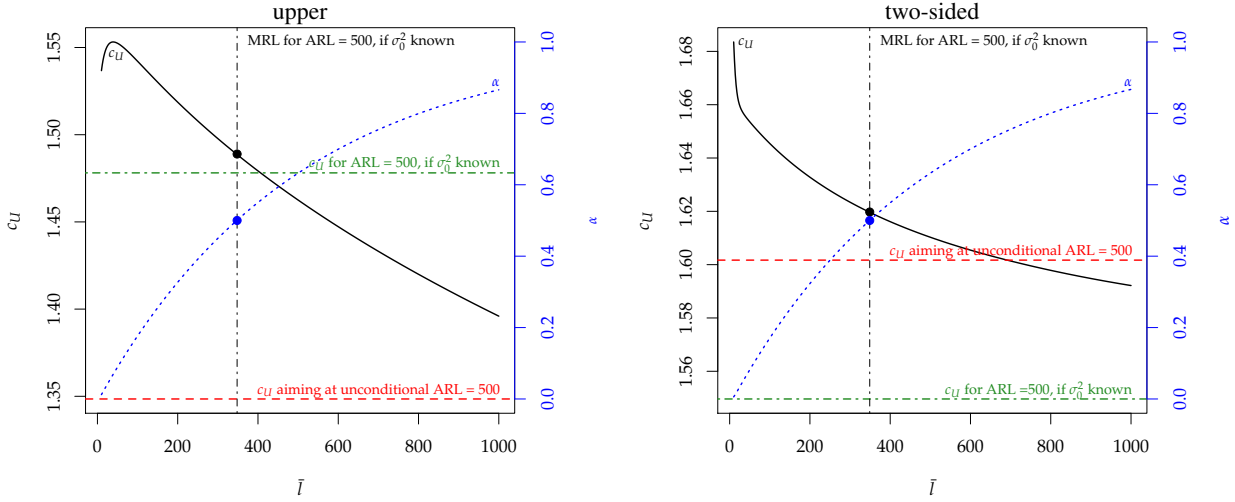


Figure 9: Choice of (\bar{l}, α) within $\alpha = P(L \leq \bar{l})$ and $E(L) = 500$ (all for known σ_0^2) and its impact on the c_U modification to secure $\alpha = P(L \leq \bar{l})$ in the case of unknown σ_0^2 , which will be estimated with a $m = 50 \times n = 5$ phase I sample.

Next, we wish to compare the detection behaviors of various values of the smoothing constant $\lambda \in \{0.05, 0.1, 0.2, 0.3\}$. In all cases, we calibrate the schemes to ensure that $P_{IC}(L \leq 10^3) = 0.25$. Again, we consider samples of size $n = 5$ and a phase I study of size $m = 50$. In Table 2 and Table 3, we provide some (unconditional) ARL values for the upper and the two-sided designs, respectively. To judge phase I's influence on the uncertainty, we compare the unconditional ARL numbers with the initial ones for a known IC variance. Interestingly, the new IC ARL results are very large but decline with increasing λ . Similar patterns can be observed in the OOC case, where for $\sigma = 1.2$, the ARL numbers are doubled. For the medium size increase, that is, $\sigma = 1.5$, the change is much smaller. Note that the order between the different EWMA designs remains stable, that is, $\lambda = 0.05$ is the best for $\sigma = 1.2$, while $\lambda = 0.1$ works best with $\sigma = 1.5$. The Shewhart S^2 chart ARL results are added, which are considerably larger than all EWMA ones.

Turning to the two-sided designs, we observe some slight differences. Most notably, the IC ARL values do not explode. Again, the OOC ARL results are tripled (1.2) and doubled (0.8) for small changes, while the increases are quite small for larger variance changes (0.5, 1.5). For the simple Shewhart chart, the unconditional ARL values nearly coincide with their known σ_0^2 counterparts (increasing σ only). For the upper and two-sided designs, the patterns in the detection ranking remain stable. For small shifts, for example, the EWMA chart with $\lambda = 0.05$ exhibits the best detection

λ	0.05	0.1	0.2	0.3	1_{Shewhart}
known σ_0^2					
c_u	1.3995	1.6453	2.0690	2.4653	5.3026
$E_1(L)$	3 444	3 461	3 470	3 473	3 476
$E_{1.2}(L)$	32.9	38.4	55.9	76.1	188.8
$E_{1.5}(L)$	8.75	8.05	8.24	9.11	19.5
phase I with $m = 50$					
c_u	1.4680	1.7198	2.1538	2.5596	5.4654
$E_1(L)$	$> 5 \times 10^9$	$> 8 \times 10^5$	47 128	21 477	8 091
$E_{1.2}(L)$	70.4	84.8	119.2	151.8	293.4
$E_{1.5}(L)$	10.6	9.52	9.79	11.0	24.0

Table 2: Unconditional ARL results for various values of λ and $P_{\text{IC}}(L \leq 10^3) = 0.25$, upper chart.

λ	0.05	0.1	0.2	0.3	1_{Shewhart}
known σ_0^2					
c_l, c_u	0.6825, 1.4377	0.5610, 1.7051	0.4146, 2.1721	0.3200, 2.6159	0.0112, 6.3542
$E_{0.5}(L)$	11.3	8.91	7.35	6.99	264
$E_{0.8}(L)$	35.3	40.5	68.0	113	1 671
$E_1(L)$	3 425	3 453	3 462	3 467	3 465
$E_{1.2}(L)$	38.9	49.0	81.1	121	639.5
$E_{1.5}(L)$	9.64	8.96	9.53	11.1	42.6
phase I with $m = 50$					
c_l, c_u	0.6377, 1.5488	0.5287, 1.8249	0.3947, 2.3077	0.3067, 2.7669	0.0111, 6.6824
$E_{0.5}(L)$	13.5	10.0	8.03	7.60	277
$E_{0.8}(L)$	75.4	93.3	151	222	1 752
$E_1(L)$	11 240	6 803	4 961	4 386	3 500
$E_{1.2}(L)$	140	173	251	328	1 094
$E_{1.5}(L)$	12.9	11.5	12.4	14.8	62.6

Table 3: Unconditional ARL results for various values of λ and $P_{\text{IC}}(L \leq 10^3) = 0.25$, two-sided chart.

performance for known and unknown IC variances. It should be stated that the Shewhart ARL performance is much worse than the EWMA ARL performance for the changes considered here.

Following the focus of this paper, we now examine the CDF profiles. Beginning with the IC versions for both designs in Figure 10, we conclude that for $l \leq \bar{l} = 1\,000$, the profiles look very similar. The $\lambda = 0.05$ line lies above all the others for these l , which changes for $l > \bar{l}$, where it features the lowest values. All other curves follow according their λ values, that is, the larger the λ , the lower the $l \leq \bar{l}$ and the higher the $l > \bar{l}$. Comparing the results for the upper and two-sided EWMA designs, we observe much steeper developments for the latter ones. In summary, we conclude that for the interesting part, namely, $l \leq \bar{l}$, the IC behavior of $P(L \leq l)$ for all considered λ values and for both design types does not really differ.

Turning to the OOC case, we start with the upper EWMA chart and two different possible new σ values, namely, the small change $\sigma_1 = 1.2$ and the medium one $\sigma_1 = 1.5$. Examining Figure 11, we observe the following stylized facts. The larger change is detected by $l \leq 100$ with probability one, while for $\sigma_1 = 1.2$, we need the whole time span, that is, $l \leq 1\,000$. Recall the corresponding expected values in Table 2, which are roughly 10 for $\sigma_1 = 1.5$ for all EWMA designs, while for $\sigma_1 = 1.2$, they range from 70 for $\lambda = 0.05$ to 150 for the largest $\lambda < 1$. Moreover, the order between these λ values defined by their ARL values is reflected by the $P(L \leq l)$ profiles. Similar patterns can be recognized for the two-sided designs in Figure 12, where we included the results for decreased variances. Not surprisingly, the detection performance for $\sigma_1 \in \{1.2, 1.5\}$ is weaker compared to the upper chart profiles in Figure 11. However, detecting decreases of the same relative order proceeds more quickly.

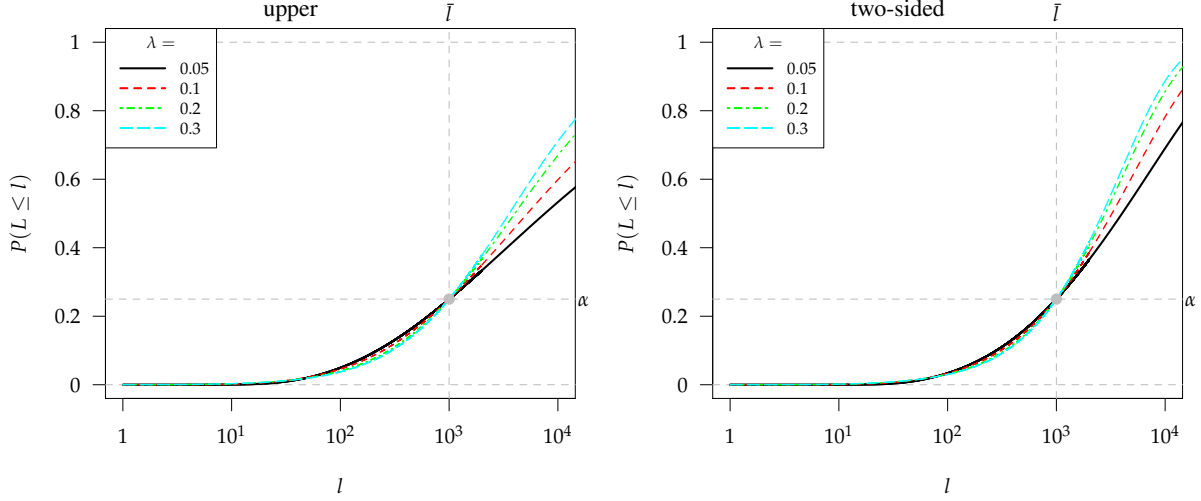


Figure 10: IC CDFs of the RL L , $P_{IC}(L \leq 10^3) = 0.25$, EWMA (various λ) S^2 ($n = 5$), $m = 50$ phase I samples.

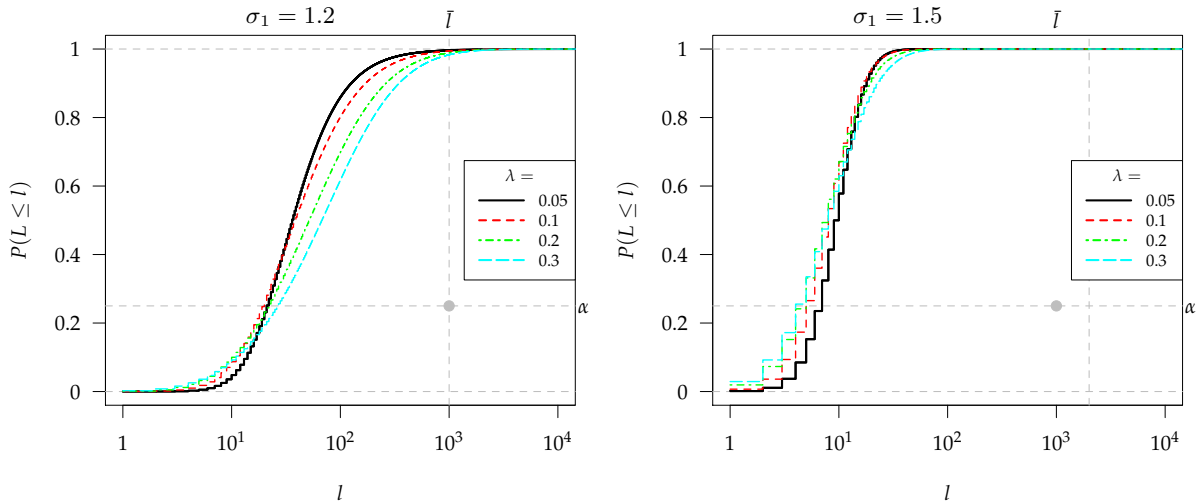


Figure 11: OOC CDFs of the RL L , $P_{IC}(L \leq 10^3) = 0.25$, upper EWMA (various λ) S^2 ($n = 5$), $m = 50$ phase I samples.

After some first glimpses of the impact of the phase I sample size, namely, m , on the magnitude of the limit modification in Figure 5, the resulting unconditional OOC ARLs in Figure 8 and the snapshots in Tables 2 and 3, some additional details will be provided here to develop recommendations regarding some lower bound for m and the choice of the smoothing constant λ . We start with the upper design and look at our selection of EWMA smoothing constants $\lambda \in \{0.05, 0.1, 0.2, 0.3\}$. In the following Figure 13, the c_u vs. phase I size m profiles are provided in two ways. First, the raw c_u limits are presented, demonstrating the typical behavior of decreasing values if $\lambda \downarrow$ or $m \uparrow$. Note that the change from $\lambda = 0.3$ to the Shewhart case ($\lambda = 1$) is really pronounced. However, the amount of widening in the control chart's continuation region done to cope with estimating the IC value of the variance is not large. Compared to the known parameter case, illustrated in Figure 13(b), we must increase the original c_u by 5 to 10% (along the λ range) for small $m < 50$ and by less than 3% for $m > 100$. The relative amount of change decreases with increasing λ . Similar results can be observed for the two-sided case. Next, we consider just the relative changes plotted in Figure 14. Except for the lower limit in the Shewhart chart, which is driven by the small sample size $n = 5$ creating difficulties while detecting variance decreases and is typically very close to zero, the profiles do not really differ from those for the one-sided case. Not surprisingly, the adjustment needed is larger than for the one-sided design. Overall, the widening of the control chart limits is about 10% or smaller for $m \geq 30$. Even some crude rule of thumb for selected values of m could be derived, such as widen the limits by 10, 8, 5, 3, 2 and 1% for $m = 20, 30, 50, 100, 200$ and 400 for the

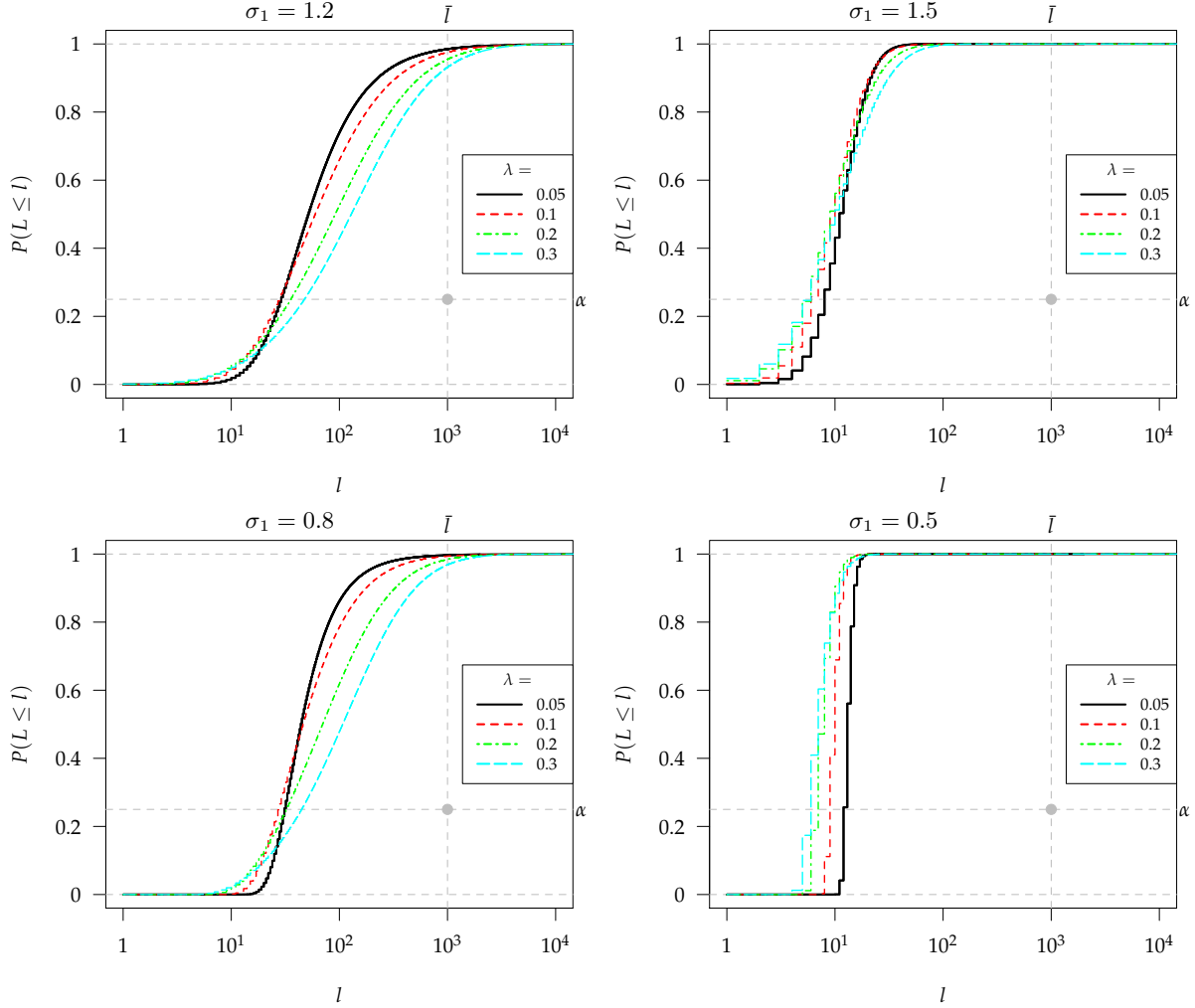


Figure 12: OOC CDFs of the RL L , $P_C(L \leq 10^3) = 0.25$, two-sided EWMA (various λ) S^2 ($n = 5$), $m = 50$ phase I samples.

phase I samples, respectively. In conclusion, utilizing the $P(L \leq \bar{l}) = \alpha$ design yields moderate changes to the control chart limits. To identify a minimum m rule or a λ guideline, we now consider the unconditional OOC ARL for two magnitudes of change.

Starting with the upper chart, we present the unconditional OOC ARL values for $\sigma_1 = 1.2$ and $\sigma_1 = 1.5$ in Figure 15 for the previously considered configurations. In Figure 15(a), we detect two segments in the ARL profiles. For small values of $m < 50$, we observe huge ARL values for all considered values of λ . In addition, the smaller the λ , the steeper the curves, which completely changes the order of the analyzed control chart designs. Given these patterns, it can be concluded that when attempting to detect small changes with an EWMA S^2 chart, phase I samples with $m \geq 50$ are definitely needed. Namely, avoiding too many false alarms for small $m < 50$ leads inevitably to the delayed detection of small changes. Things look much better for the medium-sized change $\sigma_1 = 1.5$ in Figure 15(b), where for all λ and roughly all m , the adjustment of the upper limit c_u only mildly distorts the unconditional OOC ARL. Moreover, the popular choices $\lambda = 0.1$ and $\lambda = 0.2$ produce overall decent ARL levels, indicating that a reasonable approach would be to recommend these two values, in general. Turning now to the two-sided case in Figure 16, we confirm the judgments made for the upper schemes, where again small changes create problems for $m < 50$. The good news is that for the control chart user who is interested in detecting medium-sized and large changes, the proposed adjustments of the control limits do not destroy the ability of the applied EWMA charts to detect these changes. If flagging smaller changes is of concern, a larger phase I sample size is needed, that is, $m \geq 50$, to obtain a detection performance that is comparable to that of the known parameter case. It should be noted that the ARL values for the Shewhart chart are almost always too large to be displayed in Figures 15 and 16. The one and only exception in

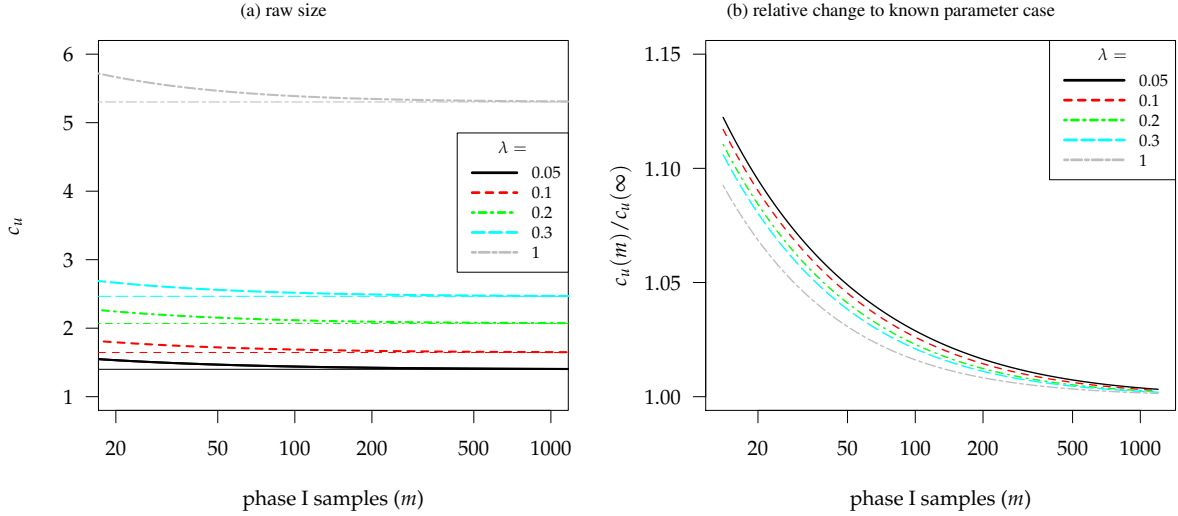


Figure 13: Modified c_u needed to achieve $P_{IC}(L \leq 10^3) = 0.25$, upper EWMA (various λ) S^2 ($n = 5$), phase I size $m = 15, 16, \dots, 1200$.

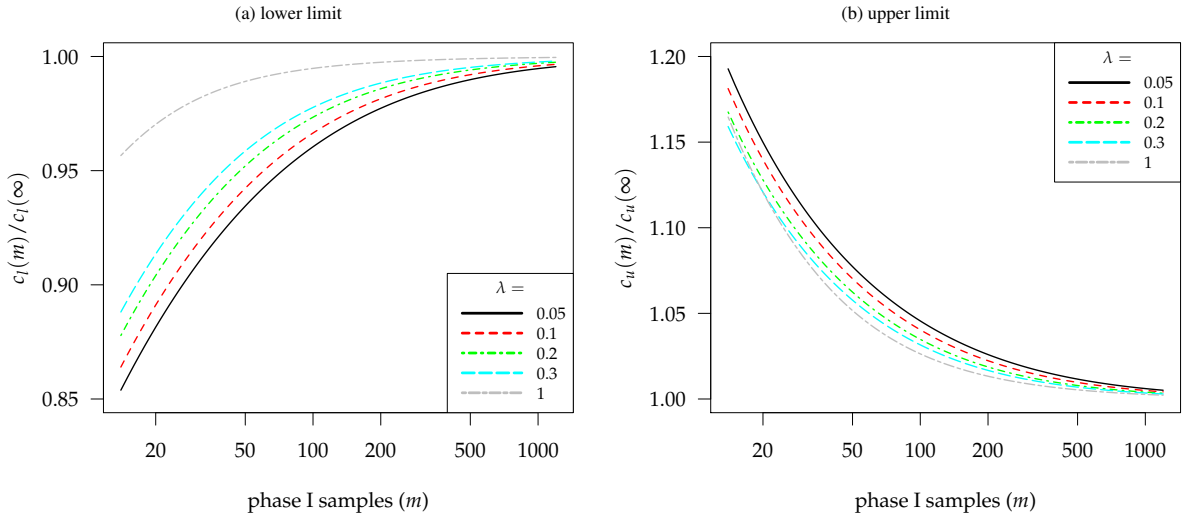


Figure 14: Ratios of the modified control limits to the original ones (known IC variance), $P_{IC}(L \leq 10^3) = 0.25$, two-sided EWMA (various λ) S^2 ($n = 5$), phase I size $m = 15, 16, \dots, 1200$.

Figure 15(a) emphasizes that detecting a small variance increase in presence of an unknown IC variance level is difficult if only $m \leq 40$ observations are available to estimate the latter value.

5 Conclusions

In order to control the false alarm behavior of EWMA S^2 charts used for monitoring a normal variance, we proposed an approach that widens the limits in a balanced way. The resulting control chart design exhibits reasonable false alarm behavior while still being able to detect medium-sized and large changes. To detect small changes, the phase I sample size must be increased to $m \geq 50$ to achieve a performance that is comparable to the known parameter case. Moreover, we believe that the notion that we are calibrating for a certain false alarm probability α within a given number of control chart values (the chart horizon \bar{l}) is easier to communicate to the statistical process monitoring community than declaring that one guarantees with probability $1 - \alpha$ that the random conditional IC ARL is at least some nominal value, which corresponds more or less directly to \bar{l} anyway. In addition, we recommend that $\lambda = 0.1$ or $= 0.2$ be used for setting up a reasonable EWMA S^2 chart. Finally, it should be noted that we have prepared an R package (available from CRAN:

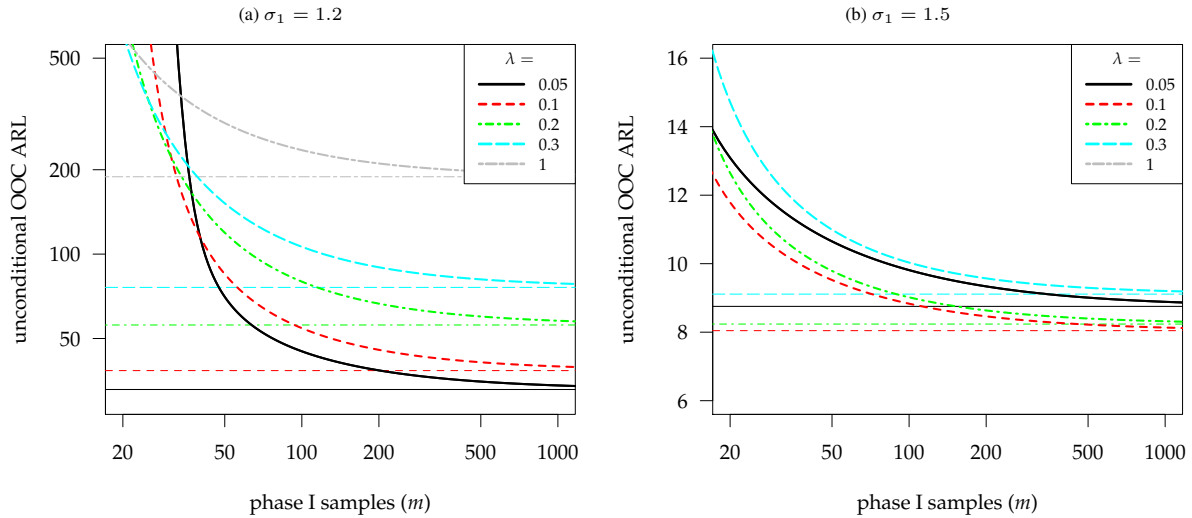


Figure 15: Unconditional OOC ARLs of the upper EWMA (various λ) S^2 ($n = 5$) charts, $P_{IC}(L \leq 10^3) = 0.25$, phase I size $m = 15, 16, \dots, 1200$.

<https://cran.r-project.org/>) that contains the functions needed to calculate the unconditional RL quantiles and ARL values as well as the control charts limits (including their adjustments for a given phase I size m). Some examples are given in the Appendix. Moreover, the shiny app <https://kassandra.hsu-hh.de/apps/knoth/s2ewmaP/> provides a more convenient access.

References

- Douglas C. Montgomery. *Statistical quality control: a modern introduction*. Wiley, Hoboken, NJ, 6. ed., internat. student version edition, 2009. ISBN 9780470233979.
- Peihua Qiu. *Introduction to statistical process control*. Chapman and Hall/CRC, 2013.
- S. W. Roberts. Control chart tests based on geometric moving averages. *Technometrics*, 1(3):239–250, 1959. doi:[10.1080/00401706.1959.10489860](https://doi.org/10.1080/00401706.1959.10489860).
- James M. Lucas and Michael S. Saccucci. Exponentially weighted moving average control schemes: Properties and enhancements. *Technometrics*, 32(1):1–12, 1990. doi:[10.1080/00401706.1990.10484583](https://doi.org/10.1080/00401706.1990.10484583).
- A. W. Wortham and L. J. Ringer. Control via exponential smoothing. *The Logistics Review*, 7(32):33–40, 1971.
- Arnold L. Sweet. Control charts using coupled exponentially weighted moving averages. *IIE Transactions*, 18(1): 26–33, 1986. doi:[10.1080/07408178608975326](https://doi.org/10.1080/07408178608975326).
- Rickie Domangue and Steven Patch. Some omnibus exponentially weighted moving average statistical process monitoring schemes. *Technometrics*, 33(3):299–313, 1991. doi:[10.1080/00401706.1991.10484836](https://doi.org/10.1080/00401706.1991.10484836).
- Stephen V. Crowder and M. D. Hamilton. An EWMA for monitoring a process standard deviation. *Journal of Quality Technology*, 24(1):12–21, 1992. doi:[10.1080/00224065.1992.11979369](https://doi.org/10.1080/00224065.1992.11979369).
- John F. MacGregor and T. J. Harris. The exponentially weighted moving variance. *Journal of Quality Technology*, 25(2):106–118, 1993. doi:[10.1080/00224065.1993.11979433](https://doi.org/10.1080/00224065.1993.11979433).
- T. C. Chang and Fah Fatt Gan. Optimal designs of one-sided EWMA charts for monitoring a process variance. *J. Stat. Comput. Simulation*, 49:33–48, 1994. doi:[10.1080/00949659408811559](https://doi.org/10.1080/00949659408811559).
- Sven Knoth. Accurate ARL computation for EWMA- S^2 control charts. *Statistics and Computing*, 15(4):341–352, 2005. doi:[10.1007/s11222-005-3393-z](https://doi.org/10.1007/s11222-005-3393-z).
- Sven Knoth. Control charting normal variance – reflections, curiosities, and recommendations. In H.-J. Lenz and P.-Th. Wilrich, editors, *Frontiers in Statistical Quality Control 9*, pages 3–18. Physica Verlag, Heidelberg, Germany, 2010. doi:[10.1007/978-3-7908-2380-6_1](https://doi.org/10.1007/978-3-7908-2380-6_1).
- L. Allison Jones, Charles W. Champ, and Steven E. Rigdon. The performance of exponentially weighted moving average charts with estimated parameters. *Technometrics*, 43(2):156–167, 2001. doi:[10.1198/004017001750386279](https://doi.org/10.1198/004017001750386279).

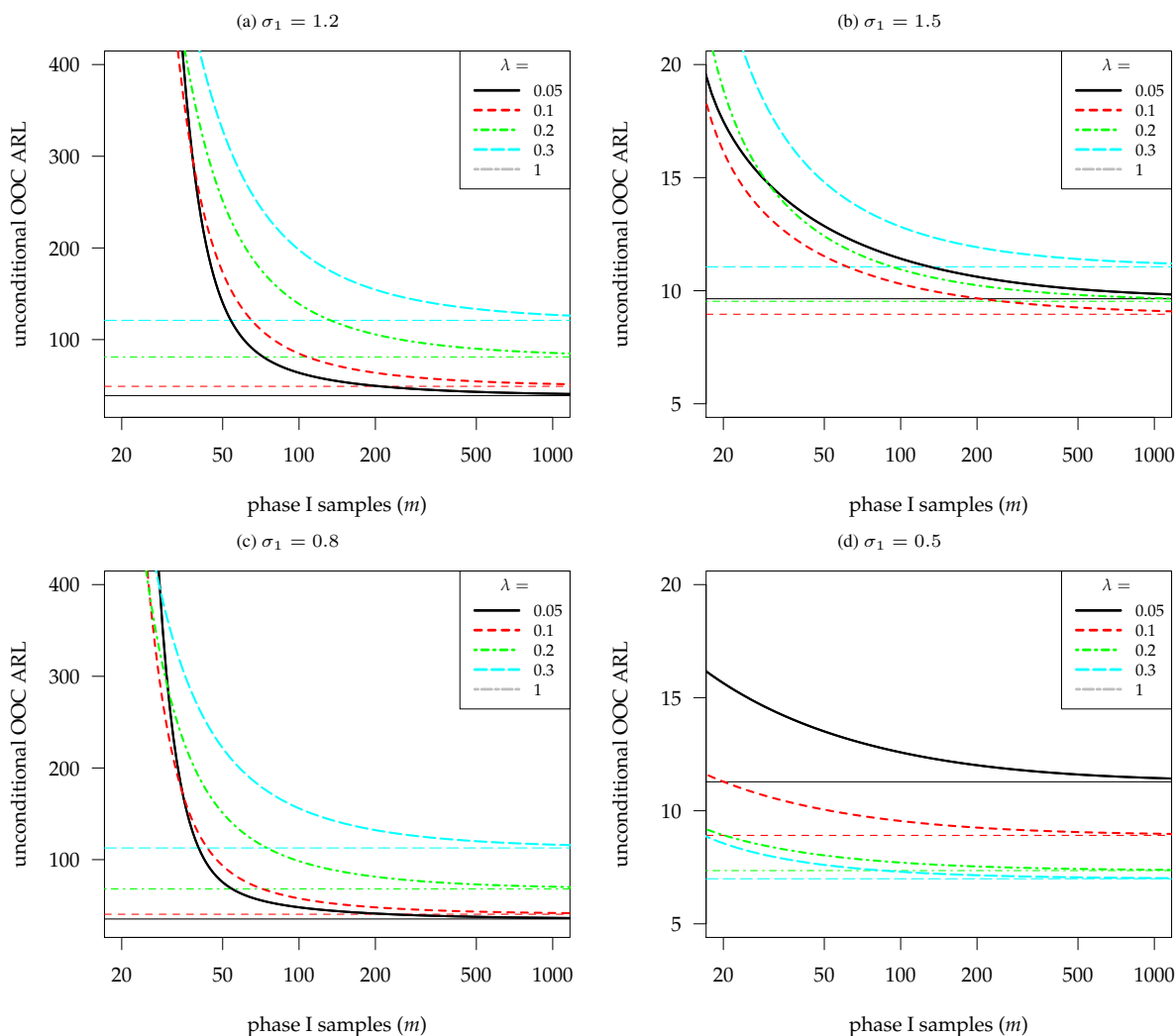


Figure 16: Unconditional OOC ARLs of the two-sided EWMA (various λ) S^2 ($n = 5$) charts, $P_{IC}(L \leq 10^3) = 0.25$, phase I size $m = 15, 16, \dots, 1200$.

Willis A. Jensen, L. Allison Jones-Farmer, Charles W. Champ, and William H. Woodall. Effects of parameter estimation on control chart properties: A literature review. *Journal of Quality Technology*, 38(4):349–364, 2006. doi:[10.1080/00224065.2006.11918623](https://doi.org/10.1080/00224065.2006.11918623).

Stelios Psarakis, Angeliki K. Vyniou, and Philippe Castagliola. Some recent developments on the effects of parameter estimation on control charts. *Quality and Reliability Engineering International*, 30(8):1113–1129, 2014. doi:[10.1002/qre.1556](https://doi.org/10.1002/qre.1556).

Willem Albers and Wilbert C. M. Kallenberg. Are estimated control charts in control? Technical Report 1569, Faculty of Mathematical Sciences, University of Twente, 2001.

Willem Albers and Wilbert C. M. Kallenberg. Estimation in Shewhart control charts: effects and corrections. *Metrika*, 59:207–234, 2004a. doi:[10.1007/s001840300280](https://doi.org/10.1007/s001840300280).

Willem Albers and Wilbert C. M. Kallenberg. Are estimated control charts in control? *Statistics: A Journal of Theoretical and Applied Statistics*, 38(1):67–79, 2004b. doi:[10.1080/02669760310001619369](https://doi.org/10.1080/02669760310001619369).

Giovanna Capizzi and Guido Masarotto. Combined Shewhart-EWMA control charts with estimated parameters. *J. Stat. Comput. Simulation*, 80(7):793–807, 2010. doi:[10.1080/00949650902773585](https://doi.org/10.1080/00949650902773585).

Mark A. Jones and Stefan H Steiner. Assessing the effect of estimation error on risk-adjusted CUSUM chart performance. *International Journal for Quality in Health Care*, 24(2):176–181, 2011. doi:[10.1093/intqhc/mzr082](https://doi.org/10.1093/intqhc/mzr082).

- Axel Gandy and Jan Terje Kvaløy. Guaranteed conditional performance of control charts via bootstrap methods. *Scandinavian Journal of Statistics*, 40(4):647–668, 2013. doi:[10.1002/sjos.12006](https://doi.org/10.1002/sjos.12006).
- Eugenio Kahn Epprecht, Lorena D. Loureiro, and Subha Chakraborti. Effect of the amount of phase I data on the phase II performance of S^2 and S control charts. *Journal of Quality Technology*, 47(2):139–155, 2015. doi:[10.1080/00224065.2015.11918121](https://doi.org/10.1080/00224065.2015.11918121).
- Baocai Guo and Bing Xing Wang. The design of the S^2 control charts based on conditional performance via exact methods. *Quality and Reliability Engineering International*, 33(7):1567–1575, 2017. doi:[10.1002/qre.2125](https://doi.org/10.1002/qre.2125).
- R. Goedhart, M. M. da Silva, M. Schoonhoven, E. K. Epprecht, S. Chakraborti, R. J. M. M. Does, and Á Veiga. Shewhart control charts for dispersion adjusted for parameter estimation. *IIE Transactions*, 49(8):838–848, 2017. doi:[10.1080/24725854.2017.1299956](https://doi.org/10.1080/24725854.2017.1299956).
- Alireza Faraz, William H. Woodall, and C. Heuchenne. Guaranteed conditional performance of the S^2 control chart with estimated parameters. *International Journal of Production Research*, 53(14):4405–4413, 2015. ISSN 1366-588X. doi:[10.1080/00207543.2015.1008112](https://doi.org/10.1080/00207543.2015.1008112).
- Alireza Faraz, Cédric Heuchenne, and Erwin Saniga. An exact method for designing Shewhart \bar{X} and S^2 control charts to guarantee in-control performance. *International Journal of Production Research*, 56(7):2570–2584, 2018. doi:[10.1080/00207543.2017.1384580](https://doi.org/10.1080/00207543.2017.1384580).
- Francisco Aparisi, Jaime Mosquera, and Eugenio K. Epprecht. Simultaneously guaranteeing the in-control and out-of-control performances of the S^2 control chart with estimated variance. *Quality and Reliability Engineering International*, 34(6):1110–1126, 2018. doi:[10.1002/qre.2311](https://doi.org/10.1002/qre.2311).
- Felipe S. Jardim, Martin G. C. Sarmiento, Subhabrata Chakraborti, and Eugenio Kahn Epprecht. Design comparison between one- and two-sided S^2 control charts with estimated parameter. In *Operations Management for Social Good*, pages 753–760. Springer International Publishing, 2019. doi:[10.1007/978-3-030-23816-2_74](https://doi.org/10.1007/978-3-030-23816-2_74).
- Giovanna Capizzi and Guido Masarotto. Guaranteed in-control control chart performance with cautious parameter learning. *Journal of Quality Technology*, 52(4):385–403, 2020. doi:[10.1080/00224065.2019.1640096](https://doi.org/10.1080/00224065.2019.1640096).
- Petros E. Maravelakis and Philippe Castagliola. An EWMA chart for monitoring the process standard deviation when parameters are estimated. *Comput. Stat. Data Anal.*, 53(7):2653–2664, 2009. doi:[10.1016/j.csda.2009.01.004](https://doi.org/10.1016/j.csda.2009.01.004).
- Inez M. Zwetsloot, Marit Schoonhoven, and Ronald J. M. M. Does. A robust phase I exponentially weighted moving average chart for dispersion. *Quality and Reliability Engineering International*, 31(6):989–999, 2015. doi:[10.1002/qre.1655](https://doi.org/10.1002/qre.1655).
- Inez M. Zwetsloot and Jimoh Olawale Ajadi. A comparison of EWMA control charts for dispersion based on estimated parameters. *Computers & Industrial Engineering*, 127:436–450, 2019. doi:[10.1016/j.cie.2018.10.034](https://doi.org/10.1016/j.cie.2018.10.034).
- Subhabrata Chakraborti. Run length distribution and percentiles: The Shewhart \bar{X} chart with unknown parameters. *Quality Engineering*, 19(2):119–127, 2007. doi:[10.1080/08982110701276653](https://doi.org/10.1080/08982110701276653).
- Emmanuel Yashchin. On the analysis and design of CUSUM-Shewhart control schemes. *IBM Journal of Research and Development*, 29(4):377–391, 1985. doi:[10.1147/rd.294.0377](https://doi.org/10.1147/rd.294.0377).
- Yajun Mei. Is average run length to false alarm always an informative criterion? *Sequential Analysis*, 27(4):354–376, 2008. doi:[10.1080/07474940802445790](https://doi.org/10.1080/07474940802445790).
- Julia Kuhn, Michel R. H. Mandjes, and Thomas Taimre. Practical aspects of false alarm control for change point detection: Beyond average run length. *Methodology and Computing in Applied Probability*, 21(1):25–42, 2019. doi:[10.1007/s11009-018-9636-1](https://doi.org/10.1007/s11009-018-9636-1).
- Hans-Joachim Mittag, Dietmar Stemmann, and Bernward Tewes. EWMA-Karten zur Überwachung der Streuung von Qualitätsmerkmalen. *Allgemeines Statistisches Archiv*, 82:327–338, 1998.
- Chern Hsoon Ng and Kenneth E. Case. Development and evaluation of control charts using exponentially weighted moving averages. *Journal of Quality Technology*, 21:242–250, 1989. doi:[10.1080/00224065.1989.11979182](https://doi.org/10.1080/00224065.1989.11979182).
- Philippe Castagliola. A new S^2 -EWMA control chart for monitoring process variance. *Quality and Reliability Engineering International*, 21:781–794, 2005. doi:[10.1002/qre.686](https://doi.org/10.1002/qre.686).
- William H. Woodall and Mahmoud A. Mahmoud. The inertial properties of quality control charts. *Technometrics*, 47(4):425–436, 2005. doi:[10.1198/004017005000000256](https://doi.org/10.1198/004017005000000256).
- Sven Knoth. Accurate ARL calculation for EWMA control charts monitoring simultaneously normal mean and variance. *Sequential Analysis*, 26(3):251–264, 2007. doi:[10.1080/07474940701404823](https://doi.org/10.1080/07474940701404823).
- Joseph J. Pignatiello, C. A. Acosta-Mejía, and B. V. Rao. The performance of control charts for monitoring process dispersion. In *4th Industrial Engineering Research Conference*, pages 320–328, 1995.

- Cesar A. Acosta-Mejía and Joseph J. Pignatiello. Monitoring process dispersion without subgrouping. *Journal of Quality Technology*, 32(2):89–102, 2000. doi:[10.1080/00224065.2000.11979981](https://doi.org/10.1080/00224065.2000.11979981).
- Werner Uhlmann. *Statistische Qualitätskontrolle. Eine Einführung*. Springer Vieweg, 1982.
- Wolf Krumbholz. Unverfälschte Spannweitekarten. *Österreichische Zeitschrift für Statistik und Informatik*, 22(3): 207–218, 1992.
- Charles W. Champ and Cynthia A. Lowry. Adjusting the S -chart for detecting both increases and decreases in the standard deviation. In *Proceedings of the Decision Sciences Institute Annual Conference, Honolulu, Hawaii, November 20-22*, volume 3, pages 2112–2114, 1994.
- Sven Knoth and Manuel Cabral Morais. On ARL-unbiased control charts. In Sven Knoth and Wolfgang Schmid, editors, *Frontiers in Statistical Quality Control 11*, pages 95–117. Springer Science + Business Media, 2015. ISBN <http://id.crossref.org/isbn/978-3-319-12355-4>. doi:[10.1007/978-3-319-12355-4_7](https://doi.org/10.1007/978-3-319-12355-4_7).
- Mahmoud A. Mahmoud, G. Robin Henderson, Eugenio Kahn Epprecht, and William H. Woodall. Estimating the standard deviation in quality-control applications. *Journal of Quality Technology*, 42(4):348–357, 2010. doi:[10.1080/00224065.2010.11917832](https://doi.org/10.1080/00224065.2010.11917832).
- Nesmaa Saleh, Mahmoud A. Mahmoud, L. Allison Jones-Farmer, Inez Zwetsloot, and William H. Woodall. Another look at the EWMA control chart with estimated parameters. *Journal of Quality Technology*, 47(4):363–382, 2015. doi:[10.1080/00224065.2015.11918140](https://doi.org/10.1080/00224065.2015.11918140).
- Karl-Heinz Waldmann. Bounds for the distribution of the run length of geometric moving average charts. *Journal of the Royal Statistical Society: Series C (Applied Statistics)*, 35(2):151–158, 1986. doi:[10.2307/2347265](https://doi.org/10.2307/2347265).
- Lianjie Shu, Wenpo Huang, Yan Sub, and Kwok-Leung Tsui. Computation of the run-length percentiles of cusum control charts under changes in variances. *J. Stat. Comput. Simulation*, 83(7):1238–1251, 2013. doi:[10.1080/00949655.2012.656643](https://doi.org/10.1080/00949655.2012.656643).
- Wenpo Huang, Lianjie Shu, Wei Jiang, and Kwo-Leung Tsui. Evaluation of run-length distribution for cusum charts under gamma distributions. *IIE Transactions*, 45(9):981–994, 2013. doi:[10.1080/0740817X.2012.705455](https://doi.org/10.1080/0740817X.2012.705455).
- Min Zhang, Fadel M. Megahed, and William H. Woodall. Exponential CUSUM charts with estimated control limits. *Quality and Reliability Engineering International*, 30(2):275–286, 2014. doi:[10.1002/qre.1495](https://doi.org/10.1002/qre.1495).

A Software implementation

The functions utilized throughout the paper are implemented in the R package `spc`. For most of the figures and tables, the corresponding R code is provided as supplementary material to this contribution. Here, some basic functions (`sewma.***.prerun()`) are described as follows.

```
install.packages("spc") # in case you have not installed the package so far

library(spc) # load the package

# configuration
df <- 5 - 1 # resulting degrees of freedom (for sample size 5)
m <- 50 # phase I size
lambda <- 0.2 # EWMA smoothing constant
ellbar <- 1000 # chart horizon
alpha <- 0.25 # false alarm probability

# control limits
clu <- sewma.q.crit.prerun(lambda, ellbar, alpha, df, m*df, sided="upper")
clu <- round(clu, digits=4)
print(clu)

# IC behavior
lMAX <- 15000 # right end of support of run length cdf
CDF <- 1 - sewma.sf.prerun(lMAX, lambda, 0, clu[2], 1, df, m*df, sided="upper")
plot(1:lMAX, CDF, type="l", xlab="l", ylab="P(L<=l)", log="x")
abline(v=ellbar, h=alpha, lty=2, col="grey")
points(ellbar, alpha, pch=19, col="grey")
```

```
# OOC behavior
SIGMA <- 1.5
CDF <- 1 - sewma.sf.prerun(lMAX, lambda, 0, clu[2], SIGMA, df, m*df, sided="upper")
plot(1:lMAX, CDF, type="l", xlab="l", ylab="P(L<=l)", log="x")
abline(v=ellbar, h=alpha, lty=2, col="grey")
points(ellbar, alpha, pch=19, col="grey")

# some unconditional ARL values
L10 <- sewma.arl.prerun(lambda, 0, clu[2], 1, df, m*df, sided="upper")
L15 <- sewma.arl.prerun(lambda, 0, clu[2], SIGMA, df, m*df, sided="upper")
print( data.frame(L10, L15), digits=3 )

## output should be two figures and ...
>      cl      cu
> 0.0000 2.1538
>      L10  L15
> arl 47128 9.79
```